Investigating the role of evaporation in dew formation under different climates using 17O-excess

Chao Tian, Wenzhe Jiao, Daniel Beysens, Kudzai Farai Kaseke, Marie-Gabrielle Medici, Fadong Li, Lixin Wang

Investigating the role of evaporation in dew formation under different climates using ^{17}O-excess

Chao Tian[a,b], Wenzhe Jiao[b], Daniel Beysens[c,d], Kudzai Farai Kaseke[b,e], Marie-Gabrielle Medici[f], Fadong Li[a,g], Lixin Wang[b*]

[a] *Key Laboratory of Ecosystem Network Observation and Modeling, Institute of Geographic Sciences and Natural Resources Research, Chinese Academy of Sciences, Beijing 100101, China*

[b] *Department of Earth Sciences, Indiana University-Purdue University Indianapolis (IUPUI), IN 46202, USA*

[c] *Physique et Mécanique des Milieux Hétérogènes, CNRS, ESPCI, PSL Research University, Sorbonne Université, Sorbonne Paris Cité, 75005 Paris, France*

[d] *OPUR, 2 rue Verderet, 75016 Paris, France*

[e] *Earth Research Institute, University of California Santa Barbara, CA 93106, USA*

[f] *LPMC, Université de Nice, CNRS-UMR 7336, 06108 Nice Cedex 2, France*

[g] *University of Chinese Academy of Sciences, Beijing 100049, China*

***Corresponding author**

Lixin Wang

Department of Earth Sciences

Indiana University-Purdue University Indianapolis (IUPUI)

Indianapolis, Indiana 46202, USA

Office phone number: 317-274-7764

Email: lxwang@iupui.edu

Abstract

With increasing aridity in many regions, dew is likely to play an increasingly important role in the ecohydrological processes in many ecosystems, especially in arid and semiarid regions. Few studies investigated the role of evaporation during dew formation and how it varies under different climate settings. ^{17}O-excess, as a new tracer, could be used to extract information of evaporation dynamics from natural water samples (e.g., precipitation, river, and lake). Therefore, to fill the knowledge gap in evaporation mechanisms during dew formation, we report the isotopic variation (δ^{2}H, δ^{18}O, δ^{17}O, and ^{17}O-excess) of dew and precipitation from three distinct climatic regions (i.e., Gobabeb in the central Namib Desert, Nice in France with Mediterranean climate, and Indianapolis in the central United States with humid continental climate). We examined whether dew formed in different climate settings was affected by different degree of evaporation using observed isotopic values and evaporation models during the formation processes, and modeled the effects of key meteorological variables (i.e., temperature and relative humidity) on ^{17}O-excess variations. The results showed that dew in Gobabeb experienced kinetic fractionation associated with evaporation under non-steady state conditions during dew formation with enriched δ^{18}O and low ^{17}O-excess values. Dew formations with temperatures over 14.7^{o}C in Indianapolis were also influenced by evaporation under non-steady state conditions. However, dew formation in Nice did not experience significant evaporation. Evaporation processes (equilibrium or kinetic fractionation) occurring during nights with heavy dew under three climate settings were mainly related to the variation of atmosphere relative humidity. The ^{17}O-excess tracer provides a new method to distinguish the different evaporation processes (equilibrium or kinetic fractionation) during dew formation and our result provides an improved understanding of dew formation.

Keywords: drylands; ecohydrology; equilibrium fractionation; kinetic fractionation; stable isotopes

1. Introduction

Dew is the condensation of water vapor into liquid droplets on a substrate when the substrate surface temperature drops below the dew point (Beysens, 2018; Monteith and Unsworth, 2013). It usually occurs at night or in early morning when reduced input of shortwave radiation results in a negative net radiation balance at the substrate. Dew occurs in most climate zones. It is an important source of moisture for epiphytes and lichens with special physical features absorbing atmospheric moisture (Gerlein-Safdi et al., 2018). Dew can reach and even exceed annual rainfall and serve as a sustainable and stable water source to maintain plant and small animal survival in arid and semiarid environments (Kidron et al., 2011; Tomaszkiewicz et al., 2015; Wang et al., 2017), especially during periods of drought. Dew could even be the only water source in a continental semiarid grassland (Aguirre-Gutiérrez et al., 2019). It is also viewed as a small but important part of the water balance in humid areas (Ritter et al., 2019; Tuller and Chilton, 1973). Dew significantly increased soil water potential such as in Namib Desert (Wang et al., 2019). It can be directly absorbed by plant roots from soil, and can reduce the evaporation loss of soil moisture to mediate water status in water-stressed plants (Aguirre-Gutiérrez et al., 2019; Munné-Bosch and Alegre, 1999). As a water source, dew can also be directly absorbed through leaves, and then alter leaf-level energy balance, reduce transpiration rate, and improve photosynthesis (Grammatikopoulos and Manetas, 1994; Guo et al., 2016; Rao et al., 2009; Zhang et al., 2019).

Air temperature and relative humidity (RH), the environmental determinants of dew deposition, are expected to change rapidly with climate change, and may affect the frequency and amount of dew deposition (Cook et al., 2014; Nepstad et al., 2008; Tomaszkiewicz et al., 2016; Vuollekoski et al., 2015). Previous studies showed that nocturnal temperatures increase with climate change, implying a lower RH and lower dew amounts in the future (Donat and Alexander, 2012; Martín et al., 2012). In a continental-scale study, it is found that the frequency of dew formation at night in the grasslands is between 15% and 95% during the study period and dew formation has a strong linear relationship with nocturnal RH (Ritter et al., 2019). Generally, when dew forms, the RH of ambient air should be high enough (>70%), and the substrate surface temperature should drop below the dew point due to radiative cooling (Lekouch et al., 2010). However, recent study showed that dew may form at lower RH as long as vapor saturation occur at the air-substrate interface (Kidron and Starinsky, 2019). For instance, a study in the semi-arid region of Loess Plateau of China indicated that dew can form when RH is around 30% (Wang and Zhang, 2011). Therefore, RH controls on dew formation may differ among climate regions. Most previous research does not consider evaporation during dew formation because it occurs during night or in early morning and evaporation is considered minimum. As a result, the role of evaporation during dew formation is not well understood. However, evaporation during dew formation has been observed in the past. For instance, evaporation during dew formation is observed during 2:00 to 4:00 am in the Loess Plateau of China leading to a decreasing dew amount (Wang and Zhang, 2011). It is also observed in Linze inland river basin (Fang and Ding, 2005). The knowledge gaps in dew evaporation during formation hinder our understanding of dew formation mechanisms and an accurate prediction of dew formation changes under future climates. Although the dew amount collected (traditional method) at sequential times at night or

96 in early morning can be used to indicate evaporation process, continuous dew recording is
97 logistically challenging and difficult to implement due to intensive labor requirement.

98 Stable isotopes of traditional hydrogen and oxygen (δ^2H and $\delta^{18}O$) are natural tracers to
99 diagnose changes in different hydrometeorological processes undergoing equilibrium and kinetic
100 fractionation during water phase change (Crawford et al., 2013; Cui et al., 2020; Soderberg et al.,
101 2012; Zhao et al., 2012). The equilibrium fractionation is determined by the saturation vapor
102 pressure. The kinetic fractionation is attributed to different diffusivities of different isotopes.
103 Generally, dew is one type of liquid condensation, supposedly dominated by equilibrium
104 fractionation. To the best of our knowledge, there is no effort examining the two fractionation
105 processes (equilibrium and kinetic fractionation) associated with evaporation during dew
106 formation. Condensation can be considered as the inverse of evaporation, with similar
107 fractionation mechanisms between vapor and liquid. As such, isotope studies on dew
108 condensation mechanism can be used to better understand the two fractionation processes
109 associated with evaporation during dew formation process. For instance, the $\delta^{18}O$ values in
110 surface dew in Brazil consistently tracked atmospheric vapor $\delta^{18}O$ values, which is generally
111 regarded as the Rayleigh equilibrium fractionation process (Zhang et al., 2009). Wen et al. (2012)
112 point out that the effect of equilibrium fractionation on the δ^2H and $\delta^{18}O$ of dew is greater than
113 that of the kinetic fractionation although humidity deviated from the saturation conditions by up
114 to 120% on the leaf surface in a cropland and a grassland in China. Deshpande et al. (2013)
115 recognize that dew could involve a certain degree of kinetic fractionation in super-saturated
116 environments at a coastal village of India. These dew formation studies, based on δ^2H and $\delta^{18}O$,
117 can distinguish equilibrium and kinetic fractionation processes. However, these studies are either
118 based on the assumption of equilibrium fractionation during condensation (Zhang et al., 2009) or

require measuring atmospheric water vapor isotopes and dew isotopes simultaneously (Deshpande et al., 2013; Wen et al., 2012).

Recent advance in spectroscopy have now enabled to obtain high-precision measurements of $\delta^{17}O$ with low natural abundance. A new hydrological tracer ^{17}O-excess became available to provide additional constraints on the mechanisms of water phase changes (Barkan and Luz, 2007). The major advantage of ^{17}O-excess over the conventional isotopes is its sole RH dependence between $10^{o}C$ to $45^{o}C$ (Barkan and Luz, 2005; Cao and Liu, 2011), which is confirmed by field observations (Landais et al., 2010; Li et al., 2017; Uechi and Uemura, 2019; Winkler et al., 2012). Recent studies also show that the relationship between $\delta'^{18}O$ and $\delta'^{17}O$ can be used to better reveal tap water and precipitation formation mechanisms (Tian et al., 2020; Tian et al., 2019), differentiate synoptic drought and local drought (Kaseke et al., 2018), and distinguish fog and dew (Kaseke et al., 2017).

According to the conceptual evaporation model, ^{17}O-excess and the relationships between different isotopic parameters (e.g., $\delta'^{18}O$ vs. $\delta'^{17}O$; ^{17}O-excess vs. $\delta'^{18}O$ (or d-excess)) can be used to infer whether water is affected by equilibrium fractionation or kinetic fractionation associated with evaporation under steady state or non-steady state (Barkan and Luz, 2005; Barkan and Luz, 2007; Criss, 1999). The evaporation model under steady state condition was based on traditional Rayleigh fractionation model. Rayleigh distillation assumes that water vapor evaporates in isotopic equilibrium condition with no additional sources or vapor recycling processes (e.g., evaporative recharge or atmospheric transport characteristics) (Fiorella et al., 2019; Winnick et al., 2014). However, most natural evaporation under non-steady state condition depends on external atmospheric vapor. Therefore, the significant difference of boundary conditions between steady-state and non-steady state models is the existence of atmospheric

142 water vapor, resulting in differently shaped evaporation trajectories (Li et al., 2015). The
143 relationships between different isotopic parameters have been used to estimate precipitation
144 evaporation processes in Africa and in the central U.S. (Landais et al., 2010; Tian et al., 2018).
145 The relationships have also been used to analyze evaporation loss of natural water bodies in the
146 Sistan Oasis, Iran (Surma et al., 2015), in central Atacama Desert, Chile (Surma et al., 2018),
147 and in western U.S. (Passey and Ji, 2019). Overall, ^{17}O-excess and the relationships between
148 different isotopic parameters are effective to explore the detailed evaporation processes.

149 Dew research has been largely confined to arid and semiarid environments (Beysens, 2018;
150 Tomaszkiewicz et al., 2015; Uclés et al., 2015). Therefore, a large knowledge gap exists to study
151 dew variability among different climatic regions (e.g., arid and humid regions in the inland and
152 near ocean) especially for evaporation. It is important to understand the environmental factors
153 influencing dew formation in different climate regions and this will better inform us how these
154 factors will affect dew formation under climate change. Here, we investigate dew and
155 precipitation isotopic variations to explore the evaporation mechanisms of dew formation in
156 three different climate settings including Gobabeb Research and Training Center (hereafter
157 Gobabeb) in the central Namib Desert with desert climate, Nice in France with Mediterranean
158 climate, and Indianapolis in the central United States with humid continental climate. We used
159 ^{17}O-excess and the relationships between δ'^{18}O and δ'^{17}O as well as between ^{17}O-excess and
160 δ'^{18}O (or d-excess) to characterize evaporation dynamics under different climate settings and
161 examined the influence of meteorological factors (e.g., temperature and RH) on isotopes.
162 Additionally, two evaporation models under steady state (i.e., Rayleigh model) and non-steady
163 state conditions were also used to verify whether dew was affected by evaporation during its
164 formation. Furthermore, the sensitivity of temperature and RH, the two important meteorological

parameters in evaporation model and the most susceptible to climate change, were also analyzed to examine their influence on dew evaporation processes under various environmental conditions.

2. Material and methods

2.1. Site description

This study was conducted in different climatic regions (Table 1). Gobabeb Research and Training Center (23.55^{o} S, 15.04^{o} E; 405 m above sea level) is located about 60 km from the South Atlantic Ocean on the outer edge of the central Namib Desert in Namibia. The mean annual temperature and mean annual relative humidity are 21.1^{o}C and 50%, respectively (Qiao et al., 2020). The annual precipitation amount is less than 20 mm (Kaseke et al., 2017). Nice (43.74^{o} N, 7.27^{o} E; 310 m above sea level) in France is situated between the Mediterranean Sea and the Alps mountains. It is Mediterranean climate associated with hot, dry summers and mild, wet winters. The minimum and maximum of average monthly temperature are 12.4^{o}C in January and 19.6^{o}C in August, respectively, with an annual average of 16.0^{o}C, based on meteorological data from 1981 to 2010 (http://www.meteofrance.com/climat/france/nice/06088001/normales). The variations of average monthly RH are from 75% in February to 80% in May, with an annual average of 78%. The mean annual precipitation is 733 mm, with over 75% of the precipitation occurring between October and the following April. Both Gobabeb and Nice are close to the ocean. Indianapolis (39.88^{o} N, 86.27^{o} W; 258 m above sea level) is an inland city in the Midwest of the United States. Detailed meteorological characteristics in Indianapolis have been described in our previous study (Tian et al., 2018). In brief, mean annual temperature, mean annual relative humidity, and precipitation are 10.2^{o}C, 69%, and 953 mm, respectively (https://www.wunderground.com). To evaluate the degree of dryness in the three sites, aridity index values were extracted from the Global Aridity Index dataset

(https://cgiarcsi.community/data/global-aridity-and-pet-database/). The Gobabeb was hyper-arid site with aridity index of 0.01. The Nice and Indianapolis were both humid sites with aridity index of 0.98 and 0.96, respectively. According to the Köppen climate classification (Geiger, 1961; Koppen, 1936), the climate in Gobabeb, Nice, and Indianapolis belongs to desert climate, Mediterranean climate, and humid continental climate, respectively.

2.2. Sample collections and isotope analysis

Event-based dew and precipitation samples were collected at each site. To reduce evaporation effects on isotopes, all of dew samples were collected before dawn at each site and stored in sealed glass vials (15 ml) for the samples in Gobabeb and Indianapolis or polyethylene bottles for the dew samples in Nice. All of the precipitation samples were collected immediately after each event or at the earliest possible time in the morning if the precipitation event was finished after midnight. Twenty-two dew samples were collected from July 2014 to June 2017 in Gobabeb. Five rainfall samples were collected in January, February, September 2014, and February 2016. Four shallow groundwaters and two deep groundwaters were also collected. Twenty-three dew samples were collected in Nice from December 2017 to April 2018. Sixty-nine dew samples and 109 precipitation samples (including 99 rainfalls and 10 snowfalls) were collected in Indianapolis from January 2017 to October 2017 and throughout 2017, respectively. All dew and precipitation samples were delivered to the IUPUI Ecohydrology Lab to measure isotopic variations using a Triple Water Vapor Isotope Analyzer (T-WVIA-45-EP; Los Gatos Research Inc. (LGR), Mountain View, CA, USA) coupled to a Water Vapor Isotope Standard Source (WVISS, LGR, Mountain View, CA, USA). The detailed operation and calibration procedures were described in details by Tian et al. (2016) and Wang et al. (2009). The main isotopic parameters reported here are: $\delta'^{18}O = 1000 \times \ln(\delta^{18}O + 1)$, $\delta'^{17}O = 1000 \times \ln(\delta^{17}O + 1)$, λ

211 = $\delta'^{18}O/\delta'^{17}O$, ^{17}O-excess = ln ($\delta^{17}O$ + 1) − 0.528 x ln ($\delta^{18}O$ + 1), d-excess = $\delta^{2}H$ – 8 x $\delta^{18}O$
212 (Barkan and Luz, 2007; Meijer and Li, 1998). Additionally, all of the isotope ratios were
213 normalized using two international water standards (Vienna Standard Mean Ocean Water
214 (VSMOW) and Standard Light Antarctic Precipitation (SLAP)) following the procedure
215 described by Steig et al. (2014) and Schoenemann et al. (2013). Furthermore, to ensure the
216 accuracy of ^{17}O-excess measurements, ^{17}O-excess values were filtered through the methods of
217 Tian et al. (Tian and Wang, 2019; Tian et al., 2018). Based on the detection criterion, the
218 precision of our instrument was <0.80‰, <0.06‰, <0.03‰, and <12 per meg (1 per meg =
219 0.001‰) for $\delta^{2}H$, $\delta^{18}O$, $\delta^{17}O$, and ^{17}O-excess, respectively, which was comparable with previous
220 studies (Berman et al., 2013; Luz and Barkan, 2010; Schoenemann et al., 2013; Steig et al.,
221 2014).

222 **2.3. Meteorological variables**

223 To examine dew formation mechanisms under different climate settings, nocturnal
224 temperature and RH were used for analysis associated with ^{17}O-excess variations. The
225 meteorological data were available at the different meteorological stations: Gobabeb:
226 http://www.sasscalweathernet.org/; Nice: https://www.infoclimat.fr/;
227 Indianapolis: https://www.wunderground.com. The download date was about October 26th,
228 November 30th, and October 23th in 2018 for the above three websites, respectively. The
229 nocturnal data in this study were screened and averaged to hourly data from 12:00 am to 6:00 am.

230 **2.4. Evaporation model description**

231 To examine whether dew under different climate settings are affected by evaporation during
232 formation, two types of evaporation models (steady state and non-steady state conditions) were
233 used in this study. Simulated isotopic values were compared with the measured values. If most of

the simulated isotopic values matched with the measured values at temperature and RH conditions close to the measurements, the model was considered as the optimal one. The choice of steady state or non-steady state evaporation model was also verified by the observed relationships between $\delta'^{18}O$ and $\delta'^{17}O$ as well as between ^{17}O-excess and $\delta'^{18}O$ (or d-excess).

2.4.1. Evaporation simulation without external moisture sources

The atomic ratio of the residual water ${}^{*}R_{end}$ under steady state condition can be calculated by the Rayleigh fractionation model as a function of ${}^{*}\alpha_{evap}$ (Criss, 1999).

$$ {}^{*}R_{end} = {}^{*}R_{start}\, f^{(1/{}^{*}\alpha_{evap}-1)} \quad , \qquad (1) $$

where ${}^{*}R_{end}$ and ${}^{*}R_{start}$ are the isotopic ratios ($H_2{}^{17}O/H_2{}^{16}O$ or $H_2{}^{18}O/H_2{}^{16}O$) of the residual water and initial water, respectively. f is the residual fraction of liquid water. ${}^{*}\alpha_{evap}$ is evaporation fractionation factor, a function of the RH during evaporation process (Barkan and Luz, 2007).

$$ {}^{*}\alpha_{evap} = {}^{*}R_W/{}^{*}R_E = \frac{{}^{*}\alpha_{diff}\,{}^{*}\alpha_{eq}\,(1-RH)}{1-{}^{*}\alpha_{eq}RH({}^{*}R_A/{}^{*}R_W)} \quad , \qquad (2) $$

where ${}^{*}\alpha_{eq}$ and ${}^{*}\alpha_{diff}$ are liquid-vapor equilibrium fractionation factor and the diffusion fractionation factor for $^{17}O/^{16}O$ or $^{18}O/^{16}O$, respectively. R_W, R_E, and R_A are the isotopic ratios of liquid, evaporating water, and air moisture, respectively. Under the steady state experimental setup, all of the water vapor comes from the evaporating water body (i.e., no external moisture source), which means $R_A = R_E$. Therefore, the above equation (2) can be simplified to (Barkan and Luz, 2007):

$$ {}^{*}\alpha_{evap} = {}^{*}\alpha_{eq}({}^{*}\alpha_{diff}(1 - RH) + RH) \quad , \qquad (3) $$

${}^{18}\alpha_{eq}$ and ${}^{2}\alpha_{eq}$ are controlled by temperature (Horita and Wesolowski, 1994):

$$ {}^{18}\alpha_{eq} = \exp[(-7.685 + (6.7123(10^3/T)) - (1.6664\,(10^6/T^2)) + (0.35041(10^9/T^3)))/10^3] \quad , \qquad (4) $$

255 $^{2}\alpha_{eq} =$

256 $\exp[(1158.8(T^3/10^9) - 1620.1\,(T^2/10^6) + 794.84(T/10^3) - 161.04 +$

257 $2.9992(10^9/T^3))/10^3]$. (5)

258 $^{17}\alpha_{eq}$ was estimated using $^{17}\alpha_{eq} = (^{18}\alpha_{eq})^{0.529}$ based on liquid-vapor equilibrium experiments

259 (Barkan and Luz, 2005). The $^{18}\alpha_{diff}$ was 1.0283, and $^{17}\alpha_{diff}$ was $(^{18}\alpha_{diff})^{0.518}$ based on molecular

260 diffusivities of water vapor in air during evaporation experiments (Barkan and Luz, 2007). $^{2}\alpha_{diff}$

261 was estimated using $^{2}\alpha_{diff} = (^{18}\alpha_{diff})^{0.88}$ from Merlivat (1978) and confirmed by Luz et al. (2009).

262 Therefore, in our study, the $^{18}\alpha_{diff}$, $^{2}\alpha_{diff}$, and $^{17}\alpha_{diff}$ were 1.0283, 1.02486, and 1.01456,

263 respectively.

264 ***2.4.2. Evaporation simulation with external moisture sources***

265 The isotopic ratios of residual water ($^{*}R_w$) under non-steady state condition can be

266 calculated by the following equation (6) (Criss, 1999):

267 $$^{*}R_w = f^{u}\left(^{*}R_w^{i} - {}^{*}R_w^{s}\right) + {}^{*}R_w^{s} \quad , \qquad (6)$$

268 where f is the residual fraction of liquid water; the exponent u is the fractionation factor as a

269 function of RH:

270 $$u = \frac{1-{}^{*}\alpha_{evap}^{0}\,(1-RH)}{{}^{*}\alpha_{evap}^{0}\,(1-RH)} \quad , \qquad (7)$$

271 where $^{*}\alpha_{evap}^{0}$ is the effective evaporation fractionation factor at 0% RH, which could be

272 calculated by equation (2). $^{*}R_w^{i}$ is the isotopic ratio of initial water. $^{*}R_w^{s}$ is the predicted isotopic

273 ratio of residual water under steady exchange with atmospheric vapor ($^{*}R_v$).

274 $$^{*}R_w^{s} = \frac{{}^{*}\alpha_{eq}\,RH\,{}^{*}R_v}{1-{}^{*}\alpha_{evap}^{0}\,(1-RH)} \quad . \qquad (8)$$

275 ${}^{*}R_v$ was not directly measured in our study. It was determined either from literature value or
276 calculated using precipitation isotopic composition and the equilibrium fractionation factor
277 between liquid and vapor, as shown in equation (9) (Barkan and Luz, 2005).

278 $$ {}^{*}\alpha_{l/v} = \frac{({}^{*}\delta O_l + 1)}{({}^{*}\delta O_v + 1)} \quad , \qquad (9) $$

279 where ${}^{*}\alpha_{l/v}$ is a temperature-dependent equilibrium fractionation factor, calculated by the equation
280 (4) and (5). ${}^{*}\delta O = ({}^{*}R_s/{}^{*}R_{ref} - 1)$, and ${}^{*}R_s$ and ${}^{*}R_{ref}$ are the isotope ratios (e.g., $^{18}O/^{16}O$ or $^{17}O/^{16}O$) of
281 the sample and reference, respectively.

282 According to the relationships between $\delta'^{18}O$ and $\delta'^{17}O$ as well as between ^{17}O-excess and
283 $\delta'^{18}O$ (or d-excess), all of the dew in Gobabeb and some of the dew in Indianapolis were affected
284 by evaporation, while those in Nice were not affected by evaporation. The evaporated dew in
285 Indianapolis were the dew that occurred when the temperature was greater than 14.7^{o}C (thirty-
286 three events, hereafter the $dew_{T\geq 14.7^{o}C}$). As for the $dew_{T\geq 14.7^{o}C}$, there were significant relationships
287 between ^{17}O-excess and $\delta'^{18}O$ (or d-excess) with higher correlation coefficients (r = -0.54 (or
288 0.48); $p < 0.01$) than the ones under lower temperature. Therefore, dew in Gobabeb and
289 Indianapolis were simulated separately using the above two evaporation models under steady
290 state and non-steady state conditions, while the dew evaporation in Nice was not simulated. For
291 each evaporation model, different boundary conditions (including different variables and
292 parameters) were simulated to search for the optimal model in terms of temperature, RH, residual
293 fraction of liquid water (f), and isotopic values of both initial water (i.e., ${}^{*}R_{start}$ or ${}^{*}R_w^i$ for steady
294 state or non-steady state) and atmospheric water vapor (${}^{*}R_v$). Different models of dew were
295 simulated through fixed mean nocturnal temperature parameter and adjusted RH during the
296 observation period. If the adjusted RH value was close to the observed mean RH value,
297 corresponding to the similarity between the simulated and observed isotopic values including

298 relationships between $\delta'^{18}O$ and $\delta'^{17}O$ as well as between ^{17}O-excess and $\delta'^{18}O$ (or d-excess), the
299 model would be considered as the optimal one.

300 Generally, isotopic value of the initial water in the model was the minimum value of all the
301 observed values for one particular site (e.g., dew in Gobabeb under non-steady state condition)
302 (Table 2). However, not all models followed the above criterion because some dew with
303 minimum values might not be affected by evaporation. If the ideal model cannot be obtained
304 using the minimum value, the relatively low value will be considered as isotopic value of the
305 initial water (e.g., $dew_{T\geq 14.7^{o}C}$ in Indianapolis under non-steady state condition). With the
306 decreasing of residual fraction of liquid water (f), the evaporation processes increased associated
307 with the enriched $\delta^{18}O$ and decreasing ^{17}O-excess, which means that f also played an important
308 role in simulating evaporation. The equilibrium fractionation factors (α_{eq}) were calculated by
309 equation (4) and (5) using average nocturnal temperature (and not daily temperature as
310 mentioned later on) because dew occurs at night.

311 The isotopic value of atmospheric water vapor was another important variable in non-steady
312 state model. The data can be deduced from previous study (e.g., dew in Gobabeb) (Uemura et al.,
313 2010). They can also be calculated by the equilibrium relationship between precipitation and
314 water vapor following equation (9) due to the lack of direct observational vapor data. The
315 equilibrium relationship has been applied in previous studies, such as for a prolonged rain event
316 and for monthly precipitation in Beijing, China (Wen et al., 2010). Fiorella et al. (2019) also
317 point out that the equilibrium assumption gives relatively accurate estimates of the isotope ratios
318 of evaporating waters in low latitudes (equatorward of 30^{o}). It is noteworthy that to obtain the
319 isotopic values of water vapor, compared with using average nocturnal temperature as mentioned
320 above, the average daily temperature was used to calculate the equilibrium fractionation factor

($\alpha_{l/v}$) as shown in Table 2. This is because the process of converting precipitation into water vapor occurs during both day and night. For the isotopic values of precipitation, some of them were from the directly collected samples, and others were from empirical Online Isotopes in Precipitation Calculator (hereafter OIPC) model. Both of them were used to calculate the water vapor to further obtain optimal models in Gobabeb and Indianapolis. The ^{17}O-excess of local atmospheric vapor was assumed to be 33 per meg based on the global meteoric water (Luz and Barkan, 2010) because the OIPC data only include δ^2H and δ^{18}O. Additionally, for dew in Gobabeb, the mean isotopic values of measured meteoric water included not only local rainfall but also the shallow groundwater and deep groundwater.

2.5. Temperature and RH sensitivity analysis

To further explore the role of temperature and RH on ^{17}O-excess variations of dew, we used the evaporation model under non-steady state mentioned above to simulate the effects of temperature and RH on ^{17}O-excess in Gobabeb and Indianapolis (only $dew_{T\geq 14.7^{o}C}$ was used for the Indianapolis site since they are affected by evaporation).

For the sensitivity of temperature, for both of the sites, the temperature from 1.4^{o}C (the minimum nocturnal value) to 30.0^{o}C including the maximum nocturnal value (21.4^{o}C) were used to include all of the conditions for dew formation. For each site, the average nocturnal temperature and the observed minimum and maximum values for dew were also simulated to test the temperature sensitivity. For the sensitivity of RH, RH ranging from 18% to 98% with every 10% interval was used in the two sites, which include the optimal RH 78% in Gobabeb and 98% in Indianapolis as stated in the above optimal model. The other boundary conditions were assumed constant by using parameters (e.g., $^{*}R^{i}_{w}$, $^{*}R_{v}$, and f) from the optimal model.

3. Results

3.1. Meteorological characteristics of dew days

There were different nocturnal temperature and RH ranges under three different climate settings during the observation periods (Fig. 1). The average temperature in Nice was the lowest (9.1^{o}C) with the smallest range (3.6^{o}C to 15.3^{o}C), and the average in Indianapolis was the highest (13.9^{o}C) with the largest range (1.4^{o}C to 21.4^{o}C). The temperature in Gobabeb varied from 3.5^{o}C to 16.9^{o}C with an average of 11.8^{o}C. It is notable that the average RH in Gobabeb was the lowest (78%) with the largest range values (35% to 98%), and the average in Indianapolis was the highest (92%) with the smallest range values (66% to 100%). The RH in Nice varied from 55% to 94% with an average of 80%. Additionally, for the days with $dew_{T\geq14.7^{o}C}$ in Indianapolis, the temperature varied from 14.7^{o}C to 21.4^{o}C with an average of 17.4^{o}C, and the RH varied from 66% to 99% with an average of 93%.

3.2. Dew isotope variations

A largest range of dew $\delta^{18}O$ values was observed in Nice during the study period (-16.7‰ to -0.7‰) (Fig. 2). It was close to the range in Indianapolis (-13.4‰ to 0.5‰), while the smallest range was in Gobabeb (-6.8‰ to 3.2‰). The average $\delta^{18}O$ value in Gobabeb was more enriched (-1.4‰±2.6‰) than the other two sites. The average $\delta^{18}O$ value in Nice (-7.0‰±3.8‰) was almost similar to the one in Indianapolis (-6.5‰±3.1‰), while lower than those for the $dew_{T\geq14.7^{o}C}$ in Indianapolis (-5.1‰±2.6‰). The $\delta^{2}H$ and $\delta^{17}O$ variations showed similar trends to $\delta^{18}O$ in the three sites (Fig. 2).

More variable dew ^{17}O-excess values were observed in Gobabeb (-40 to 45 per meg) (Fig. 2). The range in Nice (7 to 54 per meg) was close to the one in Indianapolis (-5 to 64 per meg). The average ^{17}O-excess value in Gobabeb (9±22 per meg) was the lowest, and the one in Nice

(34±12 per meg) was almost identical to the ones in Indianapolis for all dew events (35±11 per meg) and for dews with $dew_{T\geq 14.7^{o}C}$ (34±14 per meg) (Fig. 2). The largest range of d-excess values was observed in Gobabeb (-19.9‰ to 26.5‰), and the smallest range was in Nice (0.1‰ to 32.3‰) (Fig. 2). The range in Indianapolis was from -5.0‰ to 32.1‰. The average d-excess value in Gobabeb was the lowest (6.4‰±10.0‰). The average in Nice was the highest (18.1‰±8.8‰). The average for all dew events and for $dew_{T\geq 14.7^{o}C}$ in Indianapolis were 12.7‰±7.2‰ and 10.3‰±5.6‰, respectively.

The slope of $\delta'^{18}O$-$\delta'^{17}O$ (λ) in Gobabeb (0.5202) was smaller than that in Nice and Indianapolis (0.5268 and 0.5271) (Fig. 3). The slope of all the samples in the three sites was 0.5253. The ^{17}O-excess was negatively correlated with $\delta'^{18}O$ in Gobabeb ($r = -0.93$, $p < 0.001$) and for all the samples ($r = -0.61$, $p < 0.001$) (Fig. 4a). The ^{17}O-excess was positively correlated with d-excess ($r = 0.74$, $p < 0.001$) and the slope between ^{17}O-excess and d-excess was 1.61 per meg/‰ in Gobabeb (Fig. 4b). The ^{17}O-excess was positively correlated with d-excess ($r = 0.50$, $p < 0.001$) and the slope between ^{17}O-excess and d-excess was 0.96 per meg/‰ for all the samples. There was no relationship between ^{17}O-excess and $\delta'^{18}O$ (or d-excess) in Nice ($p > 0.05$). For all dew events in Indianapolis, there was a low negative correlation between ^{17}O-excess and $\delta'^{18}O$ ($r = -0.25$, $p = 0.037$). To probe dew evaporation in Indianapolis, dew occurring under different temperature groups were used to analyze their relationships among different isotopic variables. The results showed that λ for the $dew_{T\geq 14.7^{o}C}$ was 0.5252. The ^{17}O-excess was negatively correlated with $\delta'^{18}O$ ($r = -0.54$, $p = 0.001$) and positively correlated with d-excess ($r = 0.48$, $p = 0.004$) associated with a slope of 1.18 per meg/‰ (Fig. 5c-d). Dew with temperature below 14.7°C had the higher λ (0.5280), and there was no correlation between ^{17}O-excess and $\delta'^{18}O$ (or d-excess) ($p > 0.05$).

In order to further reveal the dew formation mechanisms, the relationships between the ^{17}O-excess and both temperature and RH were analyzed in the three sites and for all the samples. The results showed that there was no relationship between temperature and ^{17}O-excess, while positive correlation was observed between RH and ^{17}O-excess for all of the samples ($r = 0.34$, $p < 0.001$) (Fig. 6). Therefore, the difference in dew ^{17}O-excess among the three sites was mainly driven by RH differences.

3.3. Dew evaporation simulation

Hundreds of dew evaporation simulations were conducted under various boundary conditions in Gobabeb and Indianapolis under steady state and non-steady state conditions. The optimal evaporation models in Gobabeb and in Indianapolis for the $dew_{T\geq14.7}{}^{o}C$ were both attained under non-steady state condition. The detailed variables and parameters are shown in Table 2. Note that the isotopic values of atmospheric water vapor were both calculated on the basis of the equilibrium fractionation between precipitation and vapor (Barkan and Luz, 2005). As for dew in Gobabeb, the $\delta^{18}O$, $\delta^{17}O$, $\delta^{2}H$, and ^{17}O-excess of vapor were -13.305‰, -7.047‰, -102.898‰, and 0 per meg, respectively. These values produced better simulation results than those from the directly observed vapor data from the South Indian and the Southern Oceans (-15.5±2.7‰, -8.2±1.5‰, and 16 per meg for $\delta^{18}O$, $\delta^{17}O$, and ^{17}O-excess, respectively) (Uemura et al., 2010). For precipitation in Gobabeb, comparing with the isotopic values from empirical Online Isotopes in Precipitation Calculator model (-2.6±0.4‰ and -13±4‰ for $\delta^{18}O$ and $\delta^{2}H$, respectively), the mean isotopic values of measured local precipitation (including rainfall and groundwater; -3.5±6.0‰ and -25.7±41.7‰ for $\delta^{18}O$ and $\delta^{2}H$, respectively) were used to estimate $\delta^{18}O_v$ and $\delta^{2}H_v$ because it could get a better match with measured values in the model. As a result, the temperature and RH of optimal model for dew in Gobabeb were identical with those of the

measured average nocturnal values during the observation period (11.8^{o}C and 78%). The simulated λ (0.5199) was almost the same with the observed λ (0.5202) (Fig. 5a-b). The negative correlations between ^{17}O-excess and δ'^{18}O were similar for simulated and measured values (slope = -8.10 and -7.76 per meg/‰ for both) (Fig. 5a). The positive correlation between ^{17}O-excess and d-excess for the model (slope = 1.58 per meg/‰) was similar with the observed value (1.61 per meg/‰) (Fig. 5b).

As for the $dew_{T\geq14.7^{o}C}$ in Indianapolis, the δ^{18}O, δ^{17}O, δ^{2}H, and ^{17}O-excess of the vapor were -14.950‰, -7.902‰, -109.725‰, and 20 per meg, respectively. The isotopic values of precipitation were from the observed value during dew observation (-5.25‰ and -33.79‰ for δ^{18}O and δ^{2}H). Using the observed precipitation values could get better simulated values than using the OIPC values (-3.20‰ and -15.40‰). With these parameters (Table 2), RH of optimal model in Indianapolis (98%) was found close to the measured average nocturnal values (93%) (Fig. 5c-d). The modeled λ (0.5250) was close to the observed one (0.5252). The negative correlations between ^{17}O-excess and δ'^{18}O were similar for simulated and measured values (slope = -3.01 and -2.84 per meg/‰ for both) (Fig. 5c). The positive correlation between ^{17}O-excess and d-excess for the model (slope = 1.17 per meg/‰) was almost identical to the observed value (slope = 1.18 per meg/‰) (Fig. 5d).

3.4. The sensitivity of temperature and RH on dew ^{17}O-excess

In order to assess the dew ^{17}O-excess sensitivity to temperature and RH, the evaporation models mentioned above were also used to simulate the dew ^{17}O-excess responses to different environmental conditions in Gobabeb and Indianapolis. The dew ^{17}O-excess sensitivity with respect to temperature and RH is shown in Fig. 7. The results indicated the ^{17}O-excess were more sensitive to changes in RH regardless the formation sites. For instance, for dew in Gobabeb,

negative correlations were observed between ^{17}O-excess and $\delta'^{18}O$ modeled by the non-steady evaporation model. The values of λ (0.5183 to 0.5208) varied slightly with large changes in temperature (1.4°C to 30.0°C) when RH was 78% (the optimal model parameter). However, the λ values (0.5187 to 0.5252) changed more significantly with large changes in RH (18% to 98%) when temperature was 11.8°C (the average value during the study period) (Fig. 7a-b). Similarly, for the $dew_{T\geq14.7^{o}C}$ in Indianapolis, λ only varied from 0.5238 to 0.5260 with large changes in temperature (1.4°C to 30.0°C) when RH was 98%, while λ varied from 0.5227 to 0.5255 with large changes in RH (18% to 98%) when temperature was 17.4°C (Fig. 7c-d). It was worth noting that λ decreased with increasing temperature (1.4°C to 30.0°C) for dew in Gobabeb and Indianapolis with $dew_{T\geq14.7^{o}C}$, while there was no significant linear relationship between λ and RH regardless the dew formation sites.

4. Discussion

4.1. Dew evaporation mechanisms

Dew is recognized as an important contribution to the annual water balance in arid and semiarid ecosystems (Aguirre-Gutiérrez et al., 2019; Kidron et al., 2011; Tomaszkiewicz et al., 2015; Wang et al., 2017) even in humid region (Ritter et al., 2019; Tuller and Chilton, 1973). The importance of dew may be magnified in arid regions to alleviate water stress on natural ecosystems under changing climate (Rahimi et al., 2013). Dew formation obeys relatively complex phase change processes in different environments. In reality, dew formation does not always occur within a short time window but often lasts for several hours during the night or in early morning. Dew is often collected before dawn for many dew researches, but evaporation is likely to be unavoidable during dew formation. Evaporation can occur when the conditions for dew formation are not fulfilled any more, e.g., with lower relative humidity, which decreases the

dew point temperature with respect to air temperature, during wind gusts where heat exchange with air is enhanced, or rise of cloud cover, decreasing radiative cooling. In the previous studies on dew evaporation, the different fractionation processes (equilibrium or kinetic fractionation) are speculated based on the dew isotopic variations of condensation since evaporation and condensation are inverse phase-change processes (Deshpande et al., 2013; Wen et al., 2012). However, these studies did not provide direct evidence of different fractionation processes due to the lack of real-time monitoring of vapor isotopic variation. In addition, because real-time monitoring of vapor isotopic variation needs intensive labor and other logistics (e.g., instrument purchase, deployment, and power consumption), it is difficult to test dew formation mechanism at long-time scale and no research has been conducted to examine the different degrees of evaporation. In the current study, to alleviate these constraints, we used ^{17}O-excess and its relationships with other isotopic parameters (e.g., δ'^{18}O vs. δ'^{17}O; ^{17}O-excess vs. δ'^{18}O (or d-excess)) to probe whether dew is affected by equilibrium fractionation or kinetic fractionation associated with evaporation using dew from three distinct climate settings.

The largest range of dew ^{17}O-excess values was observed in arid Gobabeb with lowest average ^{17}O-excess value (9±22 per meg) and the most enriched δ^{18}O value (-1.4‰±2.6‰) than observed in other two humid regions in Nice and Indianapolis (Fig. 2). The λ value (0.5202) was the lowest in Gobabeb, which was close to the diffusive fractionation of atmospheric water vapor (0.5185) (Barkan and Luz, 2007) and close to previous study result at the same site (0.516) (Kaseke et al., 2017). There were significant correlations between ^{17}O-excess and both δ'^{18}O and d-excess in Gobabeb. The slope between ^{17}O-excess and d-excess in Gobabeb (1.61 per meg/‰) is similar to the values predicted by re-evaporation model in African monsoon rainfall (1.6 to 2.0 per meg/‰) (Landais et al., 2010). These indicated that the dew in Gobabeb might be more

susceptible to kinetic fractionation associated with evaporation at non-steady state than the other two humid regions in Nice and Indianapolis, which exerts a stronger impact on the isotopic exchange process leading to the more enriched $\delta^{18}O$ values and lower ^{17}O-excess values for Gobabeb dew. This has been confirmed by the detailed evaporation modeling as described in section 4.2 (Fig. 5).

The λ value of dew in Nice (0.5268) is close to the equilibrium fractionation exponent (0.529) of the liquid-vapor equilibrium and global meteoric water line (0.528) (Barkan and Luz, 2005; Luz and Barkan, 2010). It appears that Rayleigh distillation, which usually limits to the equilibrium processes, was the main mechanism explaining the temporal variations in the dew isotope values (Li et al., 2015; Wen et al., 2010).

For the $dew_{T\geq14.7^{o}C}$ in Indianapolis, the positive correlation between ^{17}O-excess and $\delta'^{18}O$ and the negative correlation between ^{17}O-excess and d-excess (1.18 per meg/‰) was comparable with the results of tap water in the United States (0.7 to 2.0 per meg/‰) (Li et al., 2015). Additionally, the λ value (0.5252) of the $dew_{T\geq14.7^{o}C}$ was lower than the equilibrium fractionation exponent (0.529), with relatively high RH (93%). According to the evaporation models mentioned by Li et al. (2015), if the evaporation process occurred under steady state with high RH, the λ would be high and close to the equilibrium fractionation exponent. This demonstrated that the $dew_{T\geq14.7^{o}C}$ in Indianapolis likely go through evaporation at non-steady state conditions, which is consistent with the theoretical evaporation model predictions as further discussed below.

4.2. Data-evaporation model comparison

To validate whether dew is influenced by evaporation as expected with ^{17}O-excess and $\delta^{18}O$ observations, two evaporation models under steady state based on Rayleigh model and non-steady state model were used to reproduce the observed results, which reflects different degrees

of equilibrium or kinetic fractionation associated with evaporation. To evaluate the quality of model fitting, a series of the evaporation-controlled evolution of ^{17}O-excess over δ'^{18}O (or d-excess) had been simulated with variable boundary conditions.

In our study, dew in Gobabeb and the $dew_{T\geq14.7^{o}C}$ in Indianapolis both experienced kinetic fractionation associated with evaporation under non-steady state condition. The initial water isotopic values were the observed minimum isotopic values in Gobabeb, while they were not the minimum values in Indianapolis. These indicated that all of the dew samples in Gobabeb could be included in the evaporation model and were susceptible to the evaporation, while not all of the $dew_{T\geq14.7^{o}C}$ in Indianapolis were affected by evaporation. Compared with simulated values under Rayleigh evaporation process, isotopic variation of residual water was significantly enriched during kinetic fractionation associated with evaporation process under non-steady state conditions. As for dew in Gobabeb, the observed δ^{18}O and δ^{17}O values were better matched with the simulated values under non-steady state than those under steady state. To facilitate the comparison with previous studies, the slope between ^{17}O-excess and d-excess (or δ'^{18}O) for the observed and simulated dew in Gobabeb were calculated based on linear correlations, although the significance of quadratic relationship between ^{17}O-excess and d-excess was a little higher than that of the linear relationship. The similar positive correlation between ^{17}O-excess and d-excess for the model and the observed value (1.58 per meg/‰ vs. 1.61 per meg/‰) indicated that the isotopic variations of dew in Gobabeb should mainly occur under non-steady state evaporation condition.

^{17}O-excess of water vapor in the optimal model in Gobabeb was 0 per meg as calculated from the relationship between δ^{17}O and δ^{18}O. This is a value that fits better with the observed data than using the mean value of global meteoric water 33 per meg (Luz and Barkan, 2010), which is

commonly used when direct observational data are lacking (e.g., in the Sistan Oasis, Iran (Surma et al., 2015) and in central Atacama Desert, Chile (Surma et al., 2018)). Note that our study is the first to use the calculated ^{17}O-excess values of water vapor to predict the evaporation model. It demonstrates that the mean value of global meteoric waters does not apply anywhere, especially in arid region where other water resources other than precipitation (e.g., groundwater) have also an important impact on the local water cycle. The optimal model temperature and RH values in Gobabeb are found identical to the mean nocturnal temperature and RH during the observation period (11.8^{o}C and 78%).

As for the $dew_{T\geq14.7^{o}C}$ in Indianapolis, the optimal simulated δ^{18}O and δ^{17}O values under non-steady state condition are closer to the observation than those under steady state, resulting in a simulated λ (0.5250) similar to the observed value (0.5252) (Fig. 5c-d), thus suggesting that evaporation under non-steady state condition is more appropriate during the study period. The positive relationship between ^{17}O-excess and d-excess of the optimal model closely coincides with the measured relationship (slopes 1.17 per meg/‰ vs. 1.18 per meg/‰) (Fig. 5d), which indicates that $dew_{T\geq14.7^{o}C}$ in Indianapolis with high RH (93%) experiences a certain degree of evaporation at non-steady state condition. Therefore, if RH is close to saturation (i.e., for nearly saturated air 100% relative humidity) and λ not close to the equilibrium fractionation exponent (0.529), the evaporation process is more likely to occur under non-steady state. This means that if there are two evaporation processes with same RH, the lower λ indicates that water is more susceptible to evaporation under non-steady state, a result also verified by the evaporation processes of tap waters in the U.S. (Li et al., 2015).

During the process of evaporation simulation for the $dew_{T\geq14.7^{o}C}$ in Indianapolis, the isotopic values of atmospheric water vapor, without direct measurements, were also inferred based on the

552 assumption that vapor and precipitation condensation is an equilibrium fractionation process
553 (Barkan and Luz, 2005). For the isotopic values of precipitation, the precipitation events between
554 May and September were selected and their mean value was calculated because the $dew_{T\geq 14.7^{o}C}$
555 mainly occurred during the period. The isotopic values of the measured precipitations were lower
556 than those from the OIPC model and could give better prediction. Additionally, the ^{17}O-excess of
557 water vapor in optimal model in Indianapolis was 20 per meg, which is a better value than using
558 the mean value of global meteoric waters 33 per meg (Luz and Barkan, 2010). This further
559 provides data on water vapor isotopes in Indianapolis during May and September. In
560 consequence, the RH of optimal model in Indianapolis (98%) was close to the observed average
561 nocturnal value (93%), which indicates that the optimal model at non-steady state condition can
562 basically simulate the observed values. The reason is that, during the late spring, summer, and
563 early fall, long nights and high temperature with low RH, makes evaporation more likely to
564 occur.

565 **4.3. Sensitivity of temperature and RH**

566 Although dew formation is included in many global climate models (Rosenzweig and
567 Abramopoulos, 1997), the role of evaporation during dew formation in different climatic regions,
568 especially under climate change, is not well understood. The isotope evaporation models include
569 two important meteorological parameters: temperature and RH, and both are changing rapidly
570 under climate change with increasing temperature and decreasing RH. Lower air temperature and
571 higher RH are favorable meteorological conditions for the formation of dew (Beysens, 1995; Li,
572 2002; Ye et al., 2007). But the sensitivity of the effects of temperature and RH on evaporation
573 processes (indicated by ^{17}O-excess) during the dew formation is not clear. To this end, the ^{17}O-
574 excess sensitivity analysis to temperature and RH were performed based on the different

evaporation processes under non-steady state conditions in Gobabeb and Indianapolis with the $dew_{T\geq 14.7^{o}C}$. The evaporation lines curved under non-steady states in both Gobabeb and Indianapolis (Fig. 7). For the sensitivity of temperature, the range of slope λ varied slightly by 0.0025 and 0.0022 in Gobabeb and Indianapolis, respectively. There were negative relationships between temperature and λ at both sites. The evaporation lines at both sites were clustered together and changes slightly with the increasing of temperature from 1.4°C to 30°C at the two sites. These indicated that the ^{17}O-excess and δ'^{18}O were less sensitive to temperature (from 1.4°C to 30°C), especially for ^{17}O-excess variations, which were also observed for groundwater evaporation with no detectable change in ^{17}O-excess from 18°C to 28°C in central Atacama Desert, Chile (Surma et al., 2018). Surma et al. (2015) also showed that air temperature (from 10°C to 30°C) play a minor role for the isotopic composition of evaporating water of natural water bodies in the Sistan Oasis, Iran. Notably, all of the λ (ranging from 0.5183 to 0.5208) in Gobabeb were the low, close to the diffusion fractionation (kinetic) factor for water vapor (0.518) (Barkan and Luz, 2007). However, the λ in Indianapolis (ranging from 0.5238 to 0.5260) were higher and had less departure from the global meteoric waters line (0.528) (Luz and Barkan, 2010) and equilibrium fractionation factor for water (0.529) (Barkan and Luz, 2005). The difference is possibly due to RH difference (78% vs. 98% at two sites). This indirectly confirms the importance of the RH in evaporation as further discussed below in the sensitivity analysis.

Concerning the sensitivity of RH (from 18% to 98%) under fixed temperature, with the decreasing of RH, evaporation curves tend to be more stretched (Fig. 7). This is similar to what was observed for groundwater evaporation in central Atacama Desert, Chile (RH from 25% to 65%) (Surma et al., 2018). The slope λ range of simulated dew varied widely by 0.0065 and 0.0028 for the two sites. These demonstrated that the dew ^{17}O-excess values were more sensitive

598 to the changes in RH than that in temperature regardless the location. This strengthened the view
599 that ^{17}O-excess is principally influenced by RH during 10^{o}C to 45^{o}C, which has been confirmed
600 by theoretical experiments (Barkan and Luz, 2005; Cao and Liu, 2011) and previous field
601 observations (Landais et al., 2010; Li et al., 2017; Uechi and Uemura, 2019; Winkler et al.,
602 2012). Meanwhile, this confirms that RH is the principal drivers of dew formation in the
603 evaporation model under non-steady state. Furthermore, the ^{17}O-excess for all of the dew data in
604 our study was positively correlated with RH, which is consistent with the observations in Africa
605 monsoon rainfall (Landais et al., 2010). However,^{17}O-excess has no relationship with
606 temperature, meaning that the local RH exerts an important influence on ^{17}O-excess during dew
607 evaporation under the different climate settings.

608 **5. Conclusions**

609 Dew plays an increasing important role in the ecohydrological processes in many
610 ecosystems especially under climate change. The present report is the first to study and analyze
611 whether dew is influenced by different degree of evaporation by means of ^{17}O-excess and the
612 relationships between different isotopic parameters (e.g., δ'^{18}O vs. δ'^{17}O; ^{17}O-excess vs. δ'^{18}O (or
613 d-excess)). The study has been carried out in three different sites with various climate settings
614 (Gobabeb: desert climate, Nice: Mediterranean climate, and Indianapolis: humid continental
615 climate). Mean value ^{17}O-excess of dew in hyper-arid Gobabeb (9±22 per meg) was the lowest
616 with the largest range, while they were similar in other two humid regions Nice (34±12 per meg)
617 and Indianapolis (35±11 per meg). Based on observed data and simulations, we conclude that
618 dew formation in Gobabeb experienced kinetic fractionation processes associated with
619 evaporation under non-steady state, as well as for some of the dew events with temperature over
620 14.7^{o}C in Indianapolis, while the dew formation in Nice did not experience significant

evaporation. The local RH difference is responsible for the evaporation difference (equilibrium or kinetic fractionation) of dew formation, which is also supported by the sensitivity analysis. Informed by these results, ^{17}O-excess can be considered as a useful tracer to reveal the different evaporation process (equilibrium or kinetic fractionation) during dew formation under different climate settings.

Acknowledgements

This study was supported by the Indiana University-Purdue University Indianapolis Research Support Funds Grant, the President's International Research Awards from Indiana University, U.S. National Science Foundation (EAR-1554894), and the National Science Foundation of China (42007155). We would like to thank two anonymous reviewers for their constructive comments and suggestions, which we believe significantly strengthened our manuscript.

REFERENCE

Aguirre-Gutiérrez, C.A., Holwerda, F., Goldsmith, G.R., Delgado, J., Yepez, E., Carbajal, N., Escoto-Rodríguez, M., Arredondo, J.T., 2019. The importance of dew in the water balance of a continental semiarid grassland. Journal of Arid Environments, 168: 26-35.

Barkan, E., Luz, B., 2005. High precision measurements of $^{17}O/^{16}O$ and $^{18}O/^{16}O$ ratios in H_2O. Rapid Communications in Mass Spectrometry, 19(24): 3737-3742.

Barkan, E., Luz, B., 2007. Diffusivity fractionations of $H_2{}^{16}O/H_2{}^{17}O$ and $H_2{}^{16}O/H_2{}^{18}O$ in air and their implications for isotope hydrology. Rapid Commun. Mass Spectrom., 21(18): 2999-3005.

Berman, E.S., Levin, N.E., Landais, A., Li, S., Owano, T., 2013. Measurement of $\delta^{18}O$, $\delta^{17}O$ and ^{17}O-excess in water by Off-Axis Integrated Cavity Output Spectroscopy and Isotope Ratio Mass Spectrometry. Anal. Chem., 85(21): 10392-10398.

Beysens, D., 1995. The formation of dew. Atmos. Res., 39(1-3): 215-237.

Beysens, D., 2018. Dew Water. River Publishers.

Cao, X., Liu, Y., 2011. Equilibrium mass-dependent fractionation relationships for triple oxygen isotopes. Geochim. Cosmochim. Acta, 75(23): 7435-7445.

Cook, B.I., Smerdon, J.E., Seager, R., Coats, S., 2014. Global warming and 21 st century drying. Clim. Dyn., 43(9-10): 2607-2627.

Crawford, J., Hughes, C.E., Parkes, S.D., 2013. Is the isotopic composition of event based precipitation driven by moisture source or synoptic scale weather in the Sydney Basin, Australia? Journal of Hydrology, 507: 213-226.

Criss, R.E., 1999. Principles of stable isotope distribution. Oxford University Press on Demand.

Cui, J., Tian, L., Wei, Z., Huntingford, C., Wang, P., Cai, Z., Ma, N., Wang, L., 2020. Quantifying the controls on evapotranspiration partitioning in the highest alpine meadow ecosystems. Water Resour. Res. https://doi.org/10.1029/2019WR024815.

Deshpande, R., Maurya, A., Kumar, B., Sarkar, A., Gupta, S., 2013. Kinetic fractionation of water isotopes during liquid condensation under super-saturated condition. Geochimica et Cosmochimica Acta, 100: 60-72.

Donat, M.G., Alexander, L.V., 2012. The shifting probability distribution of global daytime and night‐time temperatures. Geophys. Res. Lett., 39(14).

Fang, J., Ding, Y., 2005. Study of the condensation water and its effect factors on the Fringes of Desert Oasis. J. Glaciol. Geocryol., 27(5): 755-760.

Fiorella, R.P., West, J.B., Bowen, G.J., 2019. Biased estimates of the isotope ratios of steady‐state evaporation from the assumption of equilibrium between vapour and precipitation. Hydrol. Process.: 1-15.

Geiger, R., 1961. berarbeitete Neuausgabe von Geiger, R: Köppen-Geiger/Klima der Erde. Wandkarte (wall map), 1: 16.

Gerlein-Safdi, C., Koohafkan, M.C., Chung, M., Rockwell, F.E., Thompson, S., Caylor, K.K., 2018. Dew deposition suppresses transpiration and carbon uptake in leaves. Agricultural and Forest Meteorology, 259: 305-316.

Grammatikopoulos, G., Manetas, Y., 1994. Direct absorption of water by hairy leaves of Phlomis fruticosa and its contribution to drought avoidance. Canadian Journal of Botany, 72(12): 1805-1811.

Guo, X., Zha, T., Jia, X., Wu, B., Feng, W., Xie, J., Gong, J., Zhang, Y., Peltola, H., 2016. Dynamics of Dew in a Cold Desert-Shrub Ecosystem and Its Abiotic Controls. Atmosphere, 7(3): 32.

Horita, J., Wesolowski, D.J., 1994. Liquid-vapor fractionation of oxygen and hydrogen isotopes of water from the freezing to the critical temperature. Geochimica et Cosmochimica Acta, 58(16): 3425-3437.

Kaseke, K.F., Wang, L., Seely, M.K., 2017. Nonrainfall water origins and formation mechanisms. Sci. adv., 3(3): e1603131.
Kaseke, K.F., Wang, L., Wanke, H., Tian, C., Lanning, M., Jiao, W., 2018. Precipitation origins and key drivers of precipitation isotope (18O, 2H, and 17O) compositions over Windhoek. Journal of Geophysical Research: Atmospheres, 123(14): 7311-7330.
Kidron, G.J., Starinsky, A., 2019. Measurements and ecological implications of non-rainfall water in desert ecosystems–A Review. Ecohydrology: e2121.
Kidron, G.J., Temina, M., Starinsky, A., 2011. An investigation of the role of water (rain and dew) in controlling the growth form of lichens on cobbles in the Negev Desert. Geomicrobiology Journal, 28(4): 335-346.
Koppen, W., 1936. Das geographische system der klimat. Handbuch der klimatologie: 46.
Landais, A., Risi, C., Bony, S., Vimeux, F., Descroix, L., Falourd, S., Bouygues, A., 2010. Combined measurements of ^{17}O-excess and d-excess in African monsoon precipitation: Implications for evaluating convective parameterizations. Earth Planet. Sci. Lett., 298(1): 104-112.
Lekouch, I., Mileta, M., Muselli, M., Milimouk-Melnytchouk, I., Šojat, V., Kabbachi, B., Beysens, D., 2010. Comparative chemical analysis of dew and rain water. Atmos. Res., 95(2-3): 224-234.
Li, S., Levin, N.E., Chesson, L.A., 2015. Continental scale variation in ^{17}O-excess of meteoric waters in the United States. Geochim. Cosmochim. Acta, 164: 110-126.
Li, S., Levin, N.E., Soderberg, K., Dennis, K.J., Caylor, K.K., 2017. Triple oxygen isotope composition of leaf waters in Mpala, central Kenya. Earth and Planetary Science Letters, 468: 38-50.
Li, X., 2002. Effects of gravel and sand mulches on dew deposition in the semiarid region of China. J. Hydrol., 260(1-4): 151-160.
Luz, B., Barkan, E., 2010. Variations of $^{17}O/^{16}O$ and $^{18}O/^{16}O$ in meteoric waters. Geochimica et Cosmochimica Acta, 74(22): 6276-6286.
Luz, B., Barkan, E., Yam, R., Shemesh, A., 2009. Fractionation of oxygen and hydrogen isotopes in evaporating water. Geochim. Cosmochim. Acta, 73(22): 6697-6703.
Martín, J.L., Bethencourt, J., Cuevas-Agulló, E., 2012. Assessment of global warming on the island of Tenerife, Canary Islands (Spain). Trends in minimum, maximum and mean temperatures since 1944. Climatic Change, 114(2): 343-355.
Meijer, H., Li, W., 1998. The use of electrolysis for accurate $\delta^{17}O$ and $\delta^{18}O$ isotope measurements in water. Isotopes Environ. Health Studies, 34(4): 349-369.
Merlivat, L., 1978. Molecular diffusivities of $H_2{}^{16}O$, $HD^{16}O$, and $H_2{}^{18}O$ in gases. The Journal of Chemical Physics, 69(6): 2864-2871.
Monteith, J., Unsworth, M., 2013. Principles of environmental physics: plants, animals, and the atmosphere. Academic Press.
Munné-Bosch, S., Alegre, L., 1999. Role of dew on the recovery of water-stressed Melissa officinalis L. plants. J. Plant Physiol., 154(5-6): 759-766.
Nepstad, D.C., Stickler, C.M., Filho, B.S.-., Merry, F., 2008. Interactions among Amazon land use, forests and climate: prospects for a near-term forest tipping point. Philos. T. R. Soc. B., 363(1498): 1737-1746.
Passey, B.H., Ji, H., 2019. Triple oxygen isotope signatures of evaporation in lake waters and carbonates: A case study from the western United States. Earth Planet. Sci. Lett., 518: 1-12.
Qiao, N., Zhang, L., Huang, C., Jiao, W., Maggs‐Kölling, G., Marais, E., Wang, L., 2020. Satellite observed positive impacts of fog on vegetation. Geophys. Res. Lett.: e2020GL088428.
Rahimi, J., Ebrahimpour, M., Khalili, A., 2013. Spatial changes of extended De Martonne climatic zones affected by climate change in Iran. Theor. Appl. Climatol., 112(3-4): 409-418.

Rao, B., Liu, Y., Wang, W., Hu, C., Dunhai, L., Lan, S., 2009. Influence of dew on biomass and photosystem II activity of cyanobacterial crusts in the Hopq Desert, northwest China. Soil Biology and Biochemistry, 41(12): 2387-2393.

Ritter, F., Berkelhammer, M., Beysens, D., 2019. Dew frequency across the US from a network of in situ radiometers. Hydrol. Earth Syst. Sc., 23(2): 1179-1197.

Rosenzweig, C., Abramopoulos, F., 1997. Land-surface model development for the GISS GCM. J. Climate, 10(8): 2040-2054.

Schoenemann, S.W., Schauer, A.J., Steig, E.J., 2013. Measurement of SLAP2 and GISP $\delta^{17}O$ and proposed VSMOW-SLAP normalization for $\delta^{17}O$ and ^{17}O-excess. Rapid Commun. Mass Spectrom., 27(5): 582-590.

Soderberg, K., Good, S.P., Wang, L., Caylor, K., 2012. Stable isotopes of water vapor in the vadose zone: A review of measurement and modeling techniques. Vadose Zone Journal, 11(3).

Steig, E., Gkinis, V., Schauer, A., Schoenemann, S., Samek, K., Hoffnagle, J., Dennis, K., Tan, S., 2014. Calibrated high-precision ^{17}O-excess measurements using cavity ring-down spectroscopy with laser-current-tuned cavity resonance. Atmos. Meas. Tech., 7(8): 2421-2435.

Surma, J., Assonov, S., Bolourchi, M., Staubwasser, M., 2015. Triple oxygen isotope signatures in evaporated water bodies from the Sistan Oasis, Iran. Geophys. Res. Lett., 42(20): 8456-8462.

Surma, J., Assonov, S., Herwartz, D., Voigt, C., Staubwasser, M., 2018. The evolution of ^{17}O-excess in surface water of the arid environment during recharge and evaporation. Sci. Rep., 8(1): 4972.

Tian, C., Wang, L., 2019. Stable isotope variations of daily precipitation from 2014-2018 in the central United States. Sci. Data, 6: 190018.

Tian, C., Wang, L., Jiao, W., Li, F., Tian, F., Zhao, S., 2020. Triple isotope variations of monthly tap water in China. Sci. Data, 7(1): 1-6.

Tian, C., Wang, L., Kaseke, K.F., Bird, B.W., 2018. Stable isotope compositions ($\delta^{2}H$, $\delta^{18}O$ and $\delta^{17}O$) of rainfall and snowfall in the central United States. Sci. Rep., 8: 6712.

Tian, C., Wang, L., Novick, K.A., 2016. Water vapor $\delta^{2}H$, $\delta^{18}O$ and $\delta^{17}O$ measurements using an off-axis integrated cavity output spectrometer-sensitivity to water vapor concentration, delta value and averaging-time. Rapid Commun. Mass Spectrom., 30(19): 2077-2086.

Tian, C., Wang, L., Tian, F., Zhao, S., Jiao, W., 2019. Spatial and temporal variations of tap water ^{17}O-excess in China. Geochim. Cosmochim. Acta: 1-14.

Tomaszkiewicz, M., Abou Najm, M., Beysens, D., Alameddine, I., El-Fadel, M., 2015. Dew as a sustainable non-conventional water resource: a critical review. Environmental Reviews, 23(4): 425-442.

Tomaszkiewicz, M., Najm, M.A., Beysens, D., Alameddine, I., Zeid, E.B., El-Fadel, M., 2016. Projected climate change impacts upon dew yield in the Mediterranean basin. Sci.Total Environ., 566: 1339-1348.

Tuller, S.E., Chilton, R., 1973. The role of dew in the seasonal moisture balance of a summer-dry climate. Agricultural Meteorology, 11: 135-142.

Uclés, O., Villagarcía, L., Cantón, Y., Lázaro, R., Domingo, F., 2015. Non-rainfall water inputs are controlled by aspect in a semiarid ecosystem. Journal of Arid Environments, 113: 43-50.

Uechi, Y., Uemura, R., 2019. Dominant influence of the humidity in the moisture source region on the 17O-excess in precipitation on a subtropical island. Earth Planet. Sci. Lett., 513: 20-28.

Uemura, R., Barkan, E., Abe, O., Luz, B., 2010. Triple isotope composition of oxygen in atmospheric water vapor. Geophysical Research Letters, 37(4).

Vuollekoski, H., Vogt, M., Sinclair, V.A., Duplissy, J., Järvinen, H., Kyrö, E.-M., Makkonen, R., Petäjä, T., Prisle, N.L., Räisänen, P., 2015. Estimates of global dew collection potential on artificial surfaces. Hydrol. Earth Syst. Sc.(19): 601-613.

Wang, L., Caylor, K.K., Dragoni, D., 2009. On the calibration of continuous, high-precision $\delta^{18}O$ and $\delta^{2}H$ measurements using an off-axis integrated cavity output spectrometer. Rapid Commun. Mass Spectrom., 23(4): 530-536.

Wang, L., Kaseke, K.F., Ravi, S., Jiao, W., Mushi, R., Shuuya, T., Maggs‐Kölling, G., 2019. Convergent vegetation fog and dew water use in the Namib Desert. Ecohydrology: e2130.

Wang, L., Kaseke, K.F., Seely, M.K., 2017. Effects of non‐rainfall water inputs on ecosystem functions. WIRES. Water, 4(1): e1179.

Wang, S., Zhang, Q., 2011. Atmospheric physical characteristics of dew formation in semi-arid in loess plateau. Acta. Phys. Sin., 60(5): 059203.

Wen, X., Lee, X., Sun, X., Wang, J., Hu, Z., Li, S., Yu, G., 2012. Dew water isotopic ratios and their relationships to ecosystem water pools and fluxes in a cropland and a grassland in China. Oecologia, 168(2): 549-561.

Wen, X., Zhang, S., Sun, X., Yu, G., Lee, X., 2010. Water vapor and precipitation isotope ratios in Beijing, China. J. Geophys. Res., 115(D1).

Winkler, R., Landais, A., Sodemann, H., Dümbgen, L., Prié, F., Masson-Delmotte, V., Stenni, B., Jouzel, J., 2012. Deglaciation records of ^{17}O-excess in East Antarctica: reliable reconstruction of oceanic normalized relative humidity from coastal sites. Clim. Past, 8(1): 1-16.

Winnick, M.J., Chamberlain, C.P., Caves, J.K., Welker, J.M., 2014. Quantifying the isotopic 'continental effect'. Earth and Planetary Science Letters, 406: 123-133.

Ye, Y., Zhou, K., Song, L., Jin, J., Peng, S., 2007. Dew amounts and its correlations with meteorological factors in urban landscapes of Guangzhou, China. Atmospheric Research, 86(1): 21-29.

Zhang, X., Yang, Z., Niu, G., Wang, X., 2009. Stable water isotope simulation in different reservoirs of Manaus, Brazil, by Community Land Model incorporating stable isotopic effect. International Journal of Climatology: A Journal of the Royal Meteorological Society, 29(5): 619-628.

Zhang, Y., Hao, X., Sun, H., Hua, D., Qin, J., 2019. How Populus euphratica utilizes dew in an extremely arid region. Plant Soil: 1-16.

Zhao, L., Xiao, H., Zhou, M., Cheng, G., Wang, L., Yin, L., Ren, J., 2012. Factors controlling spatial and seasonal distributions of precipitation $\delta^{18}O$ in China. Hydrological Processes, 26(1): 143-152.

Table 1. The detailed information of the three studied sites under different climate settings.

Site	Country	Latitude (^{o})	Longitude (^{o})	Elevation (m, a.s.l)	Mean annual temperature (^{o}C)	Mean annual relative humidity (%)	Precipitation (mm)	Aridity index	Köppen climate classification
Gobabeb Research and Training Center	Namiba	-23.55	15.04	405	21.1	50	<20	0.01	Desert climate
Nice	France	43.74	7.27	310	16.0	78	733	0.98	Mediterranean climate
Indianapolis	United State	39.88	-86.27	258	10.2	69	953	0.96	Humid continental climate

Table 2. The variables and parameters of optimal evaporation models under non-steady state conditions for the dew samples in Gobabeb and Indianapolis. For Indianapolis, the samples are the ones with temperature over 14.7°C.

Variable or parameter	Dew in Gobabeb	$Dew_{T\geq 14.7^{o}C}$ in Indianapolis
$\delta^{18}O$ of initial water	-6.771	-9.164
$\delta^{2}H$ of initial water	-27.708	-56.232
$\delta^{17}O$ of initial water	-3.552	-4.813
f	0.5	0.7
$^{18}\alpha_{eq}$	1.01055	1.01001
$^{2}\alpha_{eq}$	1.09455	1.08745
$^{17}\alpha_{eq}$	1.00557	1.00528
$^{18}\alpha_{diff}$	1.02830	1.02830
$^{2}\alpha_{diff}$	1.02486	1.02486
$^{17}\alpha_{diff}$	1.01456	1.01456
Average nocturnal temperature	11.8	17.4
Average nocturnal relative humidity	78	93
Simulated relative humidity	78	98
Average daily temperature	18.6	19.2
$^{18}\alpha_{l/v}$	1.00990	1.00985
$^{2}\alpha_{l/v}$	1.08600	1.08529
$^{17}\alpha_{l/v}$	1.00523	1.00520
$\delta^{18}O$ of precipitation	-3.533	-5.248
$\delta^{2}H$ of precipitation	-25.743	-33.791
$\delta^{17}O$ of precipitation	-1.857	-2.745
$\delta^{18}O$ of atmospheric water vapor	-13.305	-14.950
$\delta^{2}H$ of atmospheric water vapor	-102.898	-109.725
$\delta^{17}O$ of atmospheric water vapor	-7.047	-7.902
$\delta^{17}O$-excess of atmospheric water vapor	0	20

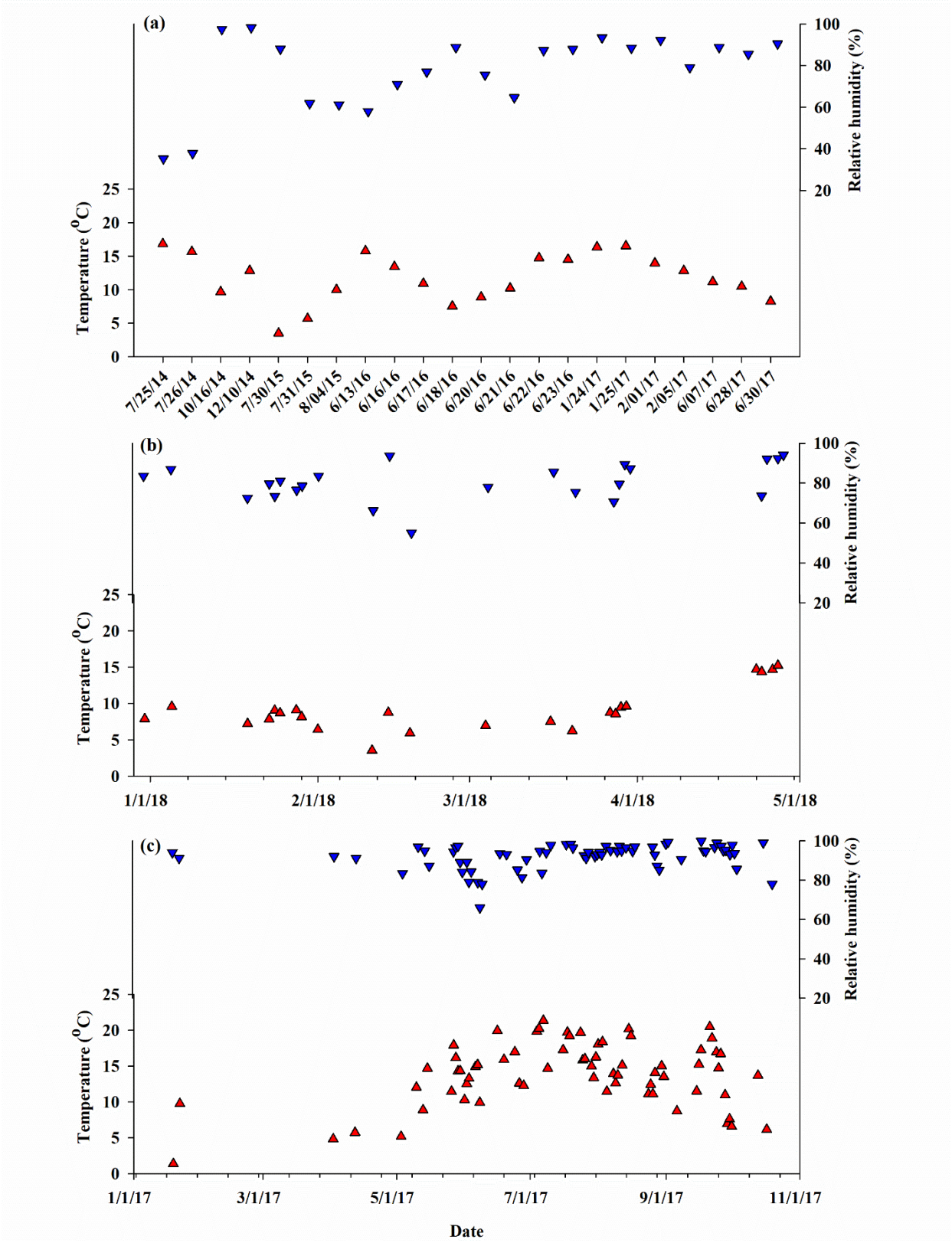

Figure 1. Daily nocturnal average temperature and relatively humidity at Gobabeb (a), Nice (b), and Indianapolis (c).

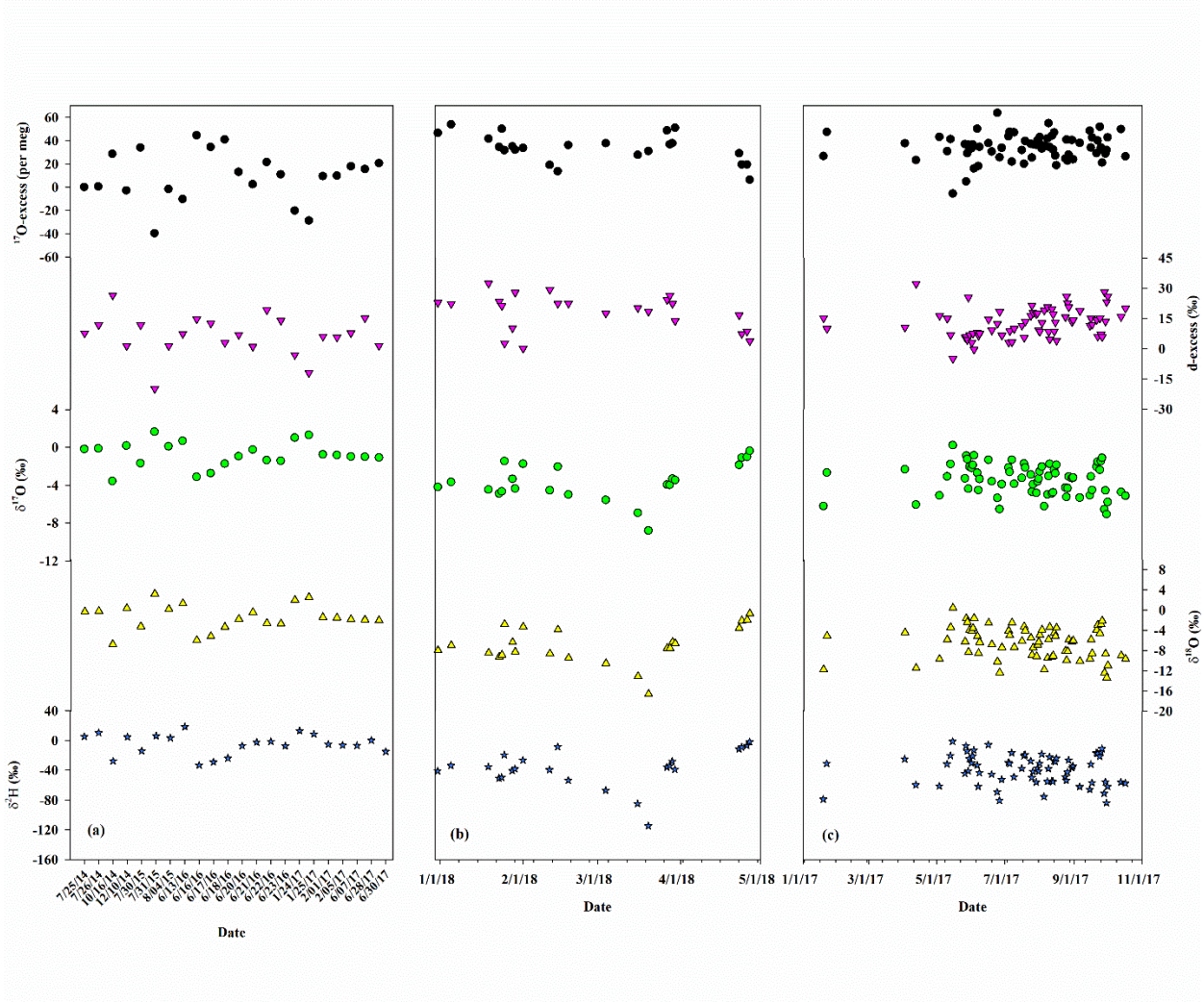

Figure 2. Dew stable isotope variations at Gobabeb (a), Nice (b), and Indianapolis (c). From top to bottom: ^{17}O-excess, d-excess, δ^{17}O, δ^{18}O, and δ^{2}H.

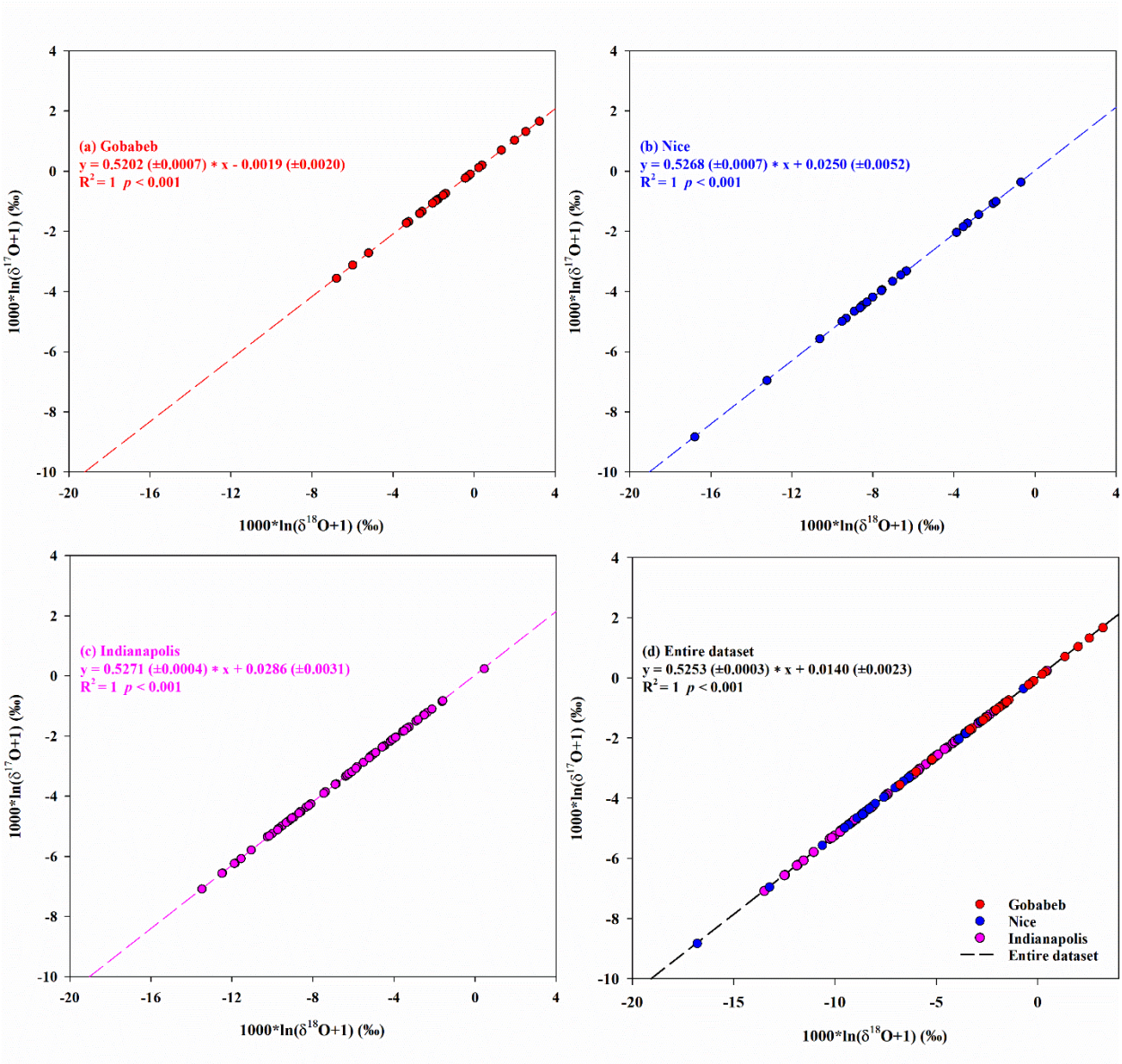

Figure 3. The relationships between $\delta^{17}O$ and $\delta^{18}O$ based on daily dew at Gobabeb (a), Nice (b), Indianapolis (c), and all of the three sites (d).

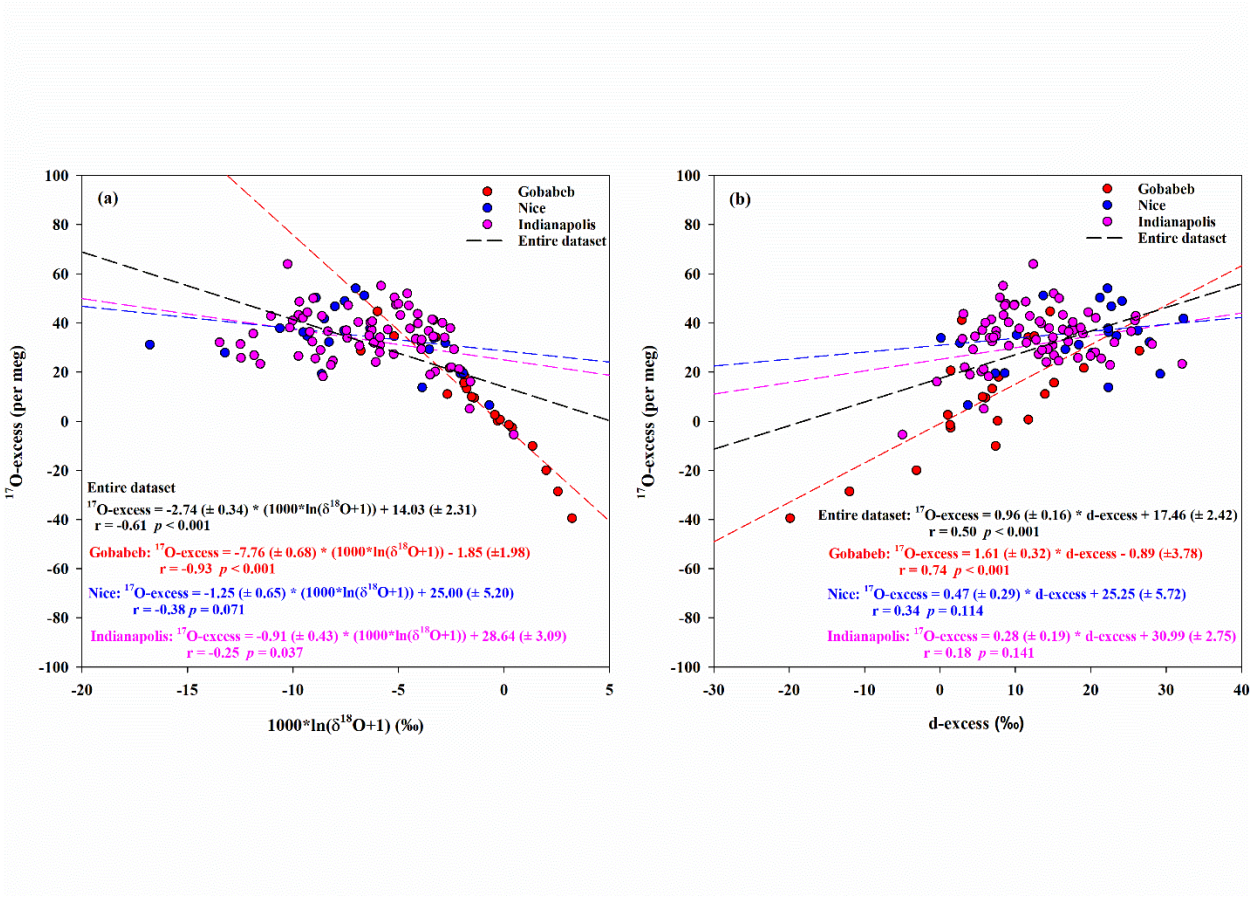

Figure 4. The relationships between ^{17}O-excess and both δ^{18}O (a) and d-excess (b) based on daily dew at Gobabeb, Nice, and Indianapolis.

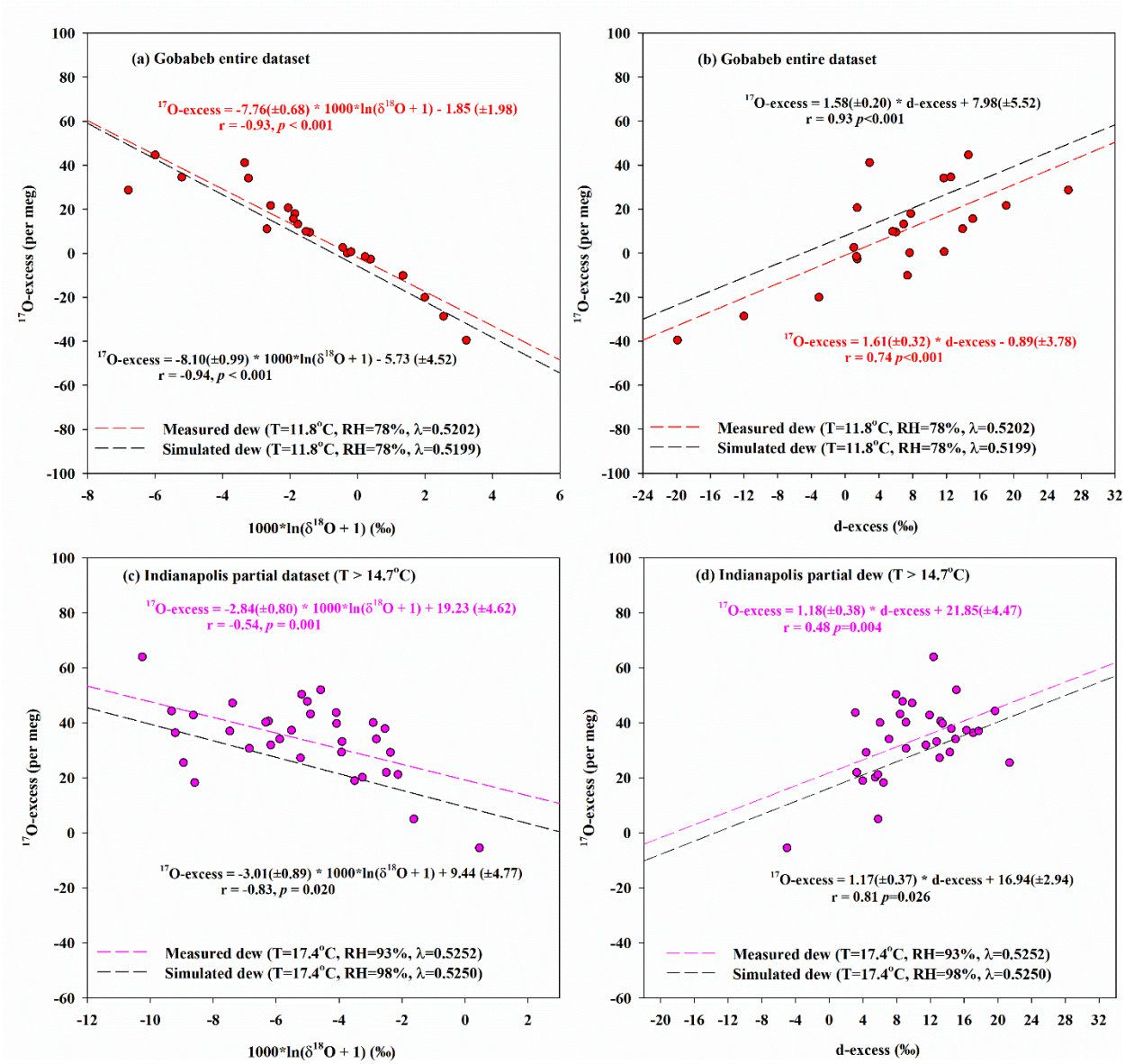

Figure 5. Modeled isotopic evolution of different sources at Gobabeb (a-b), and Indianapolis (c-d) in comparison to measured dew isotopic compositions.

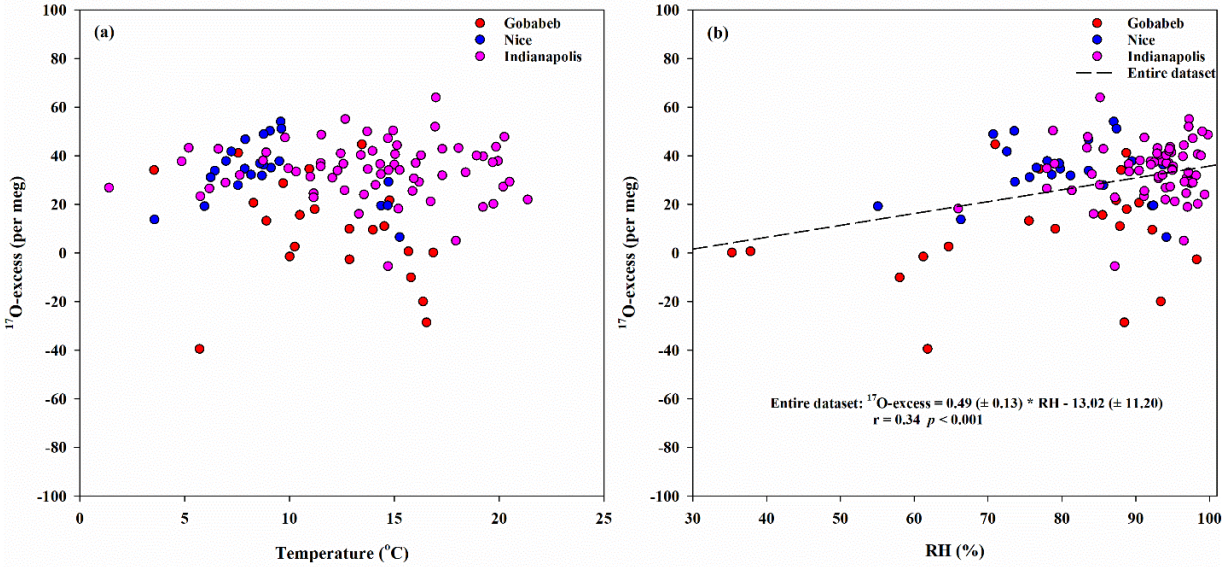

Figure 6. The relationships between ^{17}O-excess and both temperature (a) and relative humidity (b) based on daily dew at Gobabeb, Nice, and Indianapolis.

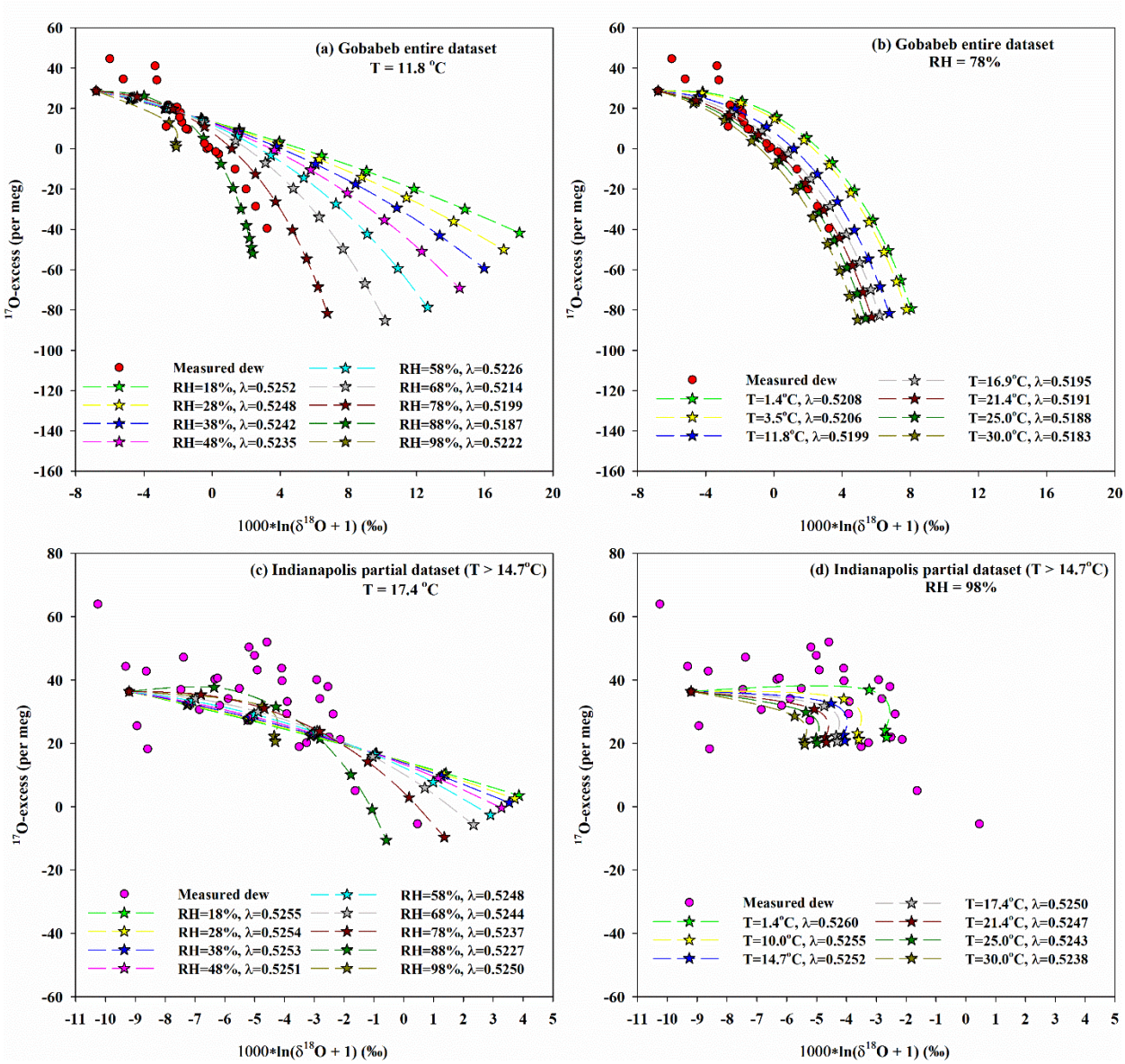

Figure 7. Modeled isotopic values (star) in Gobabeb and Indianapolis under different temperature and relative humidity in comparison to measured dew isotopic compositions (circle).